Egypt. J. Chem. **Vol. 65**, No. 9 pp. 211 - 217 (2022)

Egyptian Journal of Chemistry

http://ejchem.journals.ekb.eg/

Synthesis of new imidazole derivatives dyes and application in dye sensitized solar cells supported by DFT

Saifaldeen Fahim Abdulhussein,[a] Saifaldeen Muwafag Abdalhadi,[b*] Haitham Dalol Hanoon.[a]

[a]*Department of Chemistry, College of Science, University of Kerbala, Kerbala, Iraq*

[b]*Department of Remote Sensing, College of Remote Sensing and Geophysics, Al-Karkh University of Science, Baghdad, Iraq.*

Abstract

In this work, four free metal-organic dyes were synthesized as a donor-π bridge-acceptor system in a one-pot condensation reaction and were used as sensitizers in DSSCs. To explore the effect of substituents of the efficiency of the DSSCs, three different types of substituents were applied at the –NH position on the imidazole ring: nitrobenzene, alkyl chain and phenyl coded (PP2, PP3 and, PP4) respectively. All these dyes are characterized by ^{1}H NMR, ^{13}C NMR, UV-Vis, and mass spectroscopy. The energy band gap and structures of all dyes were estimated *via* applied tools of computational based on the density functional theory method (DFT). The dye PP3 with the alkyl chain substitution displayed the highest power conversion efficiency (PCE) of 2.01% (Jsc = 3.75 mA cm-2, Voc = 0.73 mV, FF = 73.9%) while the PP2 dye with the nitrobenzene substitution showed the lowest energy gap (2.55 eV) and lowest PCE 0.96% (Jsc = 1.59 mA cm-2, Voc = 0.080 mV, FF = 61.6%).

Keywords: photovoltaics, DSSCs, organic dyes, DFT, and imidazole derivatives.

1. Introduction

In recent years, the development of semiconductor compounds has got significant attention by researchers communities, and industries due to their application in many optoelectronic devices such as photovoltaic (PV) [1-3], molecular sensors [4, 5], organic light-emitting diodes (OLEDs) [6, 7], organic field-effect transistors (OFETs) [8, 9] and others. Many types of semiconductors are used in the optoelectronic fields, and organic dyes are one of the most important semiconductors that used in these fields and particularly in PV due to their variety of synthetic ways, lower cost, lightweight, and environmentally friendly [10, 11]. Among these benefits, organic dyes are successfully used in dye sensitized solar cells (DSSCs) and achieved 14.3% efficiency by using organic sensitizer (E)-2-cyano-3-[5-[5-[5-[5-(9-ethylcarbazol-3-yl)-3-hexylthiophen-2-yl]-3-hexylthiophen-2-yl]-3-hexylthiophen-2-yl]-3-hexylthiophen-2-yl]-N-(4-trimethoxysilylphenyl) prop-2-enamide (ADEKA-1)[12-14]. The structure of DSSC is consists of five parts; the first part is a working electrode and is made from nanoparticles of semiconductor material (TiO_2 or ZnO) with specific properties such as high surface area, high porosity, high conductivity, and high stability. The second part is transparent conducting oxide and should have high conductivity and high transparency such as ITO or FTO. The third part is the counter electrode and is usually made from metal with specific properties such as high surface area and high stability. The fourth part is electrolyte system with stable redox material such as iodine redox couple I^-/I_3^-. The last part is a photosensitizer and usually used organic compound with a special design.[15-18] The design and optoelectronic properties of organic dyes are played the main role in the efficiency of the DSSCs for an instant, the dye should be designed from three parts, donor, π-bridge, and acceptor, also other properties should be presented in the organic dye such as low energy gap (less than 3.0 eV), absorb in visible to near IR region, LUMO level of the dye should be higher the conduction band of the nano-semiconductors (TiO_2) and HOMO level should be lower the redox mediator part.[19-22] The major drawbacks of used organic dyes in DSSCs are related to the lower power conversion efficiency (PCE) due to their aggregation of the molecules on the surface of the semiconductor and that lead to inhibit the active layer (dye) to generate the electrons from incident light. Furthermore, dye aggregation has increased the recombination between the surface of the TiO_2 (CB band) and redox solution (I^-/I_3^-).[23, 24]

*Corresponding author e-mail: saifaldeen.f@uokerbala.edu.iq

Received date 07 January 2022; revised date 25 January 2022; accepted date 05 February 2022DOI: 10.21608/EJCHEM.2022.115059.5221

Among the variety of organic dye, imidazole based sensitizer are usually used in DSSCs due to their several properties, for instant, the imidazole has a conjugated chain which is lead to improve the transition of charge between donor and acceptor, also the imidazole ring could be a decrease of charge recombination after injection the electron on the surface and that is because of decreasing the density of positive charge by delocalizing the electron on the imidazole ring.[25-29]

In this study, we design and synthesize four new imidazole derivatives dyes and then used them as a dye in DSSCs. All these dyes were synthesized by using a one-pot reaction to reduce synthesis time and the cost of purifications, scheme 1 was shown the synthetic route for **PP1**, **PP2**, **PP3**, and **PP4** sensitizer.

2. Materials and methods

2.1 General information

All starting material and solvents were supplied from Alfa Aesar® and Sigma-Aldrich. The ^{1}H NMR and ^{13}C NMR were carried out on Bruker Avance III 400 and recorded at 400 MHz and 100 MHz for ^{1}H NMR and ^{13}C NMR spectra respectively. Melting point (m.p.) was obtained on a Stuart (SMP30). The FT.IR was recorded on Shimadzu (FT.IR-8400S) spectrophotometer. The UV-Vis was carried out on Shimadzu (UV-1800) spectrophotometer. Elemental analysis was recorded on a Horeaus (CHN Rapid analyzer). The mass spectroscopy was obtained on a Bruker (Micro ToF QII).

2.2 Synthesis of 4-(4,5-diphenyl-1H-imidazol-2-yl)benzoic acid (PP1)

A mixture of terephthalaldehydic acid 0.75 g (5.0 mmol), benzyl 1.0 g (5.0 mmol), ammonium acetate 0.38 g (5.0 mmol) and iodine 0.12 g (0.5 mmol) were added in 7.0 mL of ethanol and the mixture was stirred at 75 ℃ for 11 hr. The reaction was monitored by TLC and after reaction completion; the mixture was treated with $Na_2S_2O_3$ solution (5%). Afterword, the product was filtered, washed by diethyl ether and dichloromethane (two times) and then dried under vacuum, the last the product was recrystallized from hot ethanol affording **PP1**, 76% as a light yellow powder. m.p. 264-266 ℃. ^{1}H NMR δ, 400 MHz, DMSO-d_6: 12.99 (s, 1H, -NH), 8.23 (d, J = 8.4 Hz, 2H, H-Ar), 8.06 (d, J = 8.4 Hz, 2H, H-Ar), 7.52-7.60 (m, 4H, H-Ar), 7.25-7.49 (m, 6H, H-Ar). ^{13}C NMR δ, 100 MHz, DMSO-d_6: 167.57, 145.00, 139.23, 136.53, 134.54, 132.97, 130.51, 130.38, 130.32, 130.15, 129.91, 128.93, 128.33, 128.08, 127.89, 127.67, 127.52, 127.18, 125.74, 125.49. FT.IR (ν, cm^{-1}): N-H (3356), O-H (٣٢٠٠-٢٤٠٠), C=O (1689), C=N (١٦٠٦). MS (EI, *m/z*): calcd. for $C_{22}H_{16}N_2O_2$: 340.1, found 340.3. Elemental analysis, calcd (CHN): C, 77.63; H, 4.74; N, 8.23, found: C, 77.21; H, 4.62; N, 8.22.

2.3 Synthesis of 4-(1-(4-nitrophenyl)-4,5-diphenyl-1H-imidazol-2-yl)benzoic acid (PP2)

A mixture of terephthalaldehydic acid 0.75 g (5.0 mmol), benzil 1.0 g (5.0 mmol), ammonium acetate 0.38 g (5.0 mmol) , 4-nitroaniline 0.69 g (5.0 mmol) and iodine 0.12 g (0.5 mmol) were added in 7.0 mL of ethanol and the mixture was stirred at 75 ℃ for 11 hr. The reaction was monitored by TLC. After reaction completion, the mixture was treated with $Na_2S_2O_3$ solution (5%). Afterword, the product was filtered, washed by diethyl ether and dichloromethane (two times) and then dried under vacuum; the last product was recrystallized from hot ethanol affording **PP2** 70% as a yellow powder. m.p. 269-271 ℃. ^{1}H NMR δ, 400 MHz, DMSO-d_6: 8.20-8.28 (m, 4H, H-Ar), 8.03-8.18 (m, 4H, H-Ar), 7.52-7.63 (m, 4H, H-Ar), 7.13-7.49 (m, 6H, H-Ar). ^{13}C NMR δ, 100 MHz, DMSO-d_6: 167.57, 157.47, 145.58, 145.00, 139.29, 134.56, 130.47, 130.32, 130.24, 130.08, 129.99, 129.82, 129.69, 128.92, 128.67, 128.59, 128.35, 128.24, 128.08, 127.61, 127.50, 127.18, 126.88, 125.50. FT.IR (ν, cm^{-1}): O-H (٣٥٠٠-٢٤٠٠), C=O (168٧), C=N (١٦٠٠), NO_2 (1535 and 1392). MS (EI, *m/z*): calcd. for $C_{28}H_{19}N_3O_4$: 461.1, found 461.3. Elemental analysis, calcd (CHN): C, 72.88; H, 4.15; N, 9.11; found: C, 72.60; H, 4.12; N, 8.98.

2.4 Synthesis of 4-(1-(2-(diethylamino)ethyl)-4,5-diphenyl-1H-imidazol-2-yl)benzoic acid (PP3)

A mixture of terephthalaldehydic acid 0.75 g (5.0 mmol), benzil 1.0 g (5.0 mmol), ammonium acetate 0.38 g (5.0 mmol), *N*1,*N*1-diethylethane-1,2-diamine 1.4 mL (5.0 mmol) and iodine 0.12 g (0.50 mmol) were added in 7.0 mL of ethanol anf the reaction was stirred at 75 ℃ for 11 hr. The mixture was monitored by TLC and after reaction completion; the mixture was treated with $Na_2S_2O_3$ solution (5%). Afterword, the product was filtered, washed by diethyl ether and dichloromethane (two times) and then dried under vacuum; the last product was recrystallized from hot ethanol affording **PP3** 68% as an orange powder. m.p. 216-219 ℃. ^{1}H NMR δ, 400 MHz, DMSO-d_6: 8.16 (d, J = 7.4 Hz, 2H, H-Ar), 7.96 (d, J = 7.4 Hz, 2H, H-Ar), 7.54-7.56 (m, 4H, H-Ar), 7.37-7.40 (m, 6H, H-Ar), 3.17-3.19 (m, 4H, -2CH_2), 3.45 (q, J = 7.1 Hz, 4H, -2C$\underline{H_2}$-CH_3),1.05 (t, J = 7.1 Hz, 6H, -2CH_3). ^{13}C NMR δ, 100 MHz, DMSO-d_6: 167.50, 146.56, 137.22, 134.96, 132.64, 131.41, 131.28, 130.82,

130.24, 130.17, 130.01, 129.93, 129.67, 129.60, 129.49, 129.12, 128.94, 128.57, 126.71, 126.55, 51.63, 46.96, 43.27, 11.80. FT.IR (*v*, cm^{-1}): O-H (3400-2400), C-H (2978), C=O (1681), C=N (1599). MS (EI, *m/z*): calcd for $C_{28}H_{29}N_3O_2$: 439.2, found 439.4. Elemental analysis, calcd (CHN): C, 76.51; H, 6.65; N, 9.56; found: C, 76.45; H, 6.67; N, 9.49.

2.4 Synthesis of 4-(1,4,5-triphenyl-1H-imidazol-2-yl)benzoic acid (PP4)

A mixture of terephthalaldehydic acid 0.75 g (5.0 mmol), benzil 1.0 g (5.0 mmol) ammonium acetate 0.38 g (5.0 mmol) , aniline 0.45 mL (5.0 mmol) and iodine 0.12 g (0.50 mmol) were dissolved in 7 mL of ethanol and the reaction was stirred at 75 ℃ for 6 hr. The reaction was monitored by TLC and after reaction completion; the mixture was treated with $Na_2S_2O_3$ solution (5%). Afterword, the product was filtered, washed by diethyl ether and dichloromethane (3 × 15 mL) and then dried under vacuum; the last product was recrystallized from hot ethanol affording **PP4** 71% as a dark yellow powder. m.p. 250-253 ℃ . ^{1}H NMR δ, 400 MHz, DMSO-d_6: 7.83 (d, *J* = 8.1 Hz, 2H, H-Ar), 7.48-7.52 (m, 4H, H-Ar), 7.24-7.35 (m, 13H, H-Ar). ^{13}C NMR *δ*, 100 MHz, DMSO-d_6: 145.46, 137.80, 136.89, 134.68, 134.63, 134.54, 132.47, 131.59, 131.51, 130.69, 130.60, 130.56, 130.47, 130.31, 130.09, 130.01, 129.76, 129.58, 129.43, 129.14, 129.03, 128.97, 128.69, 128.58. FT.IR (*v*, cm^{-1}): O-H (3400-2500), C=O (1708), C=N (1606). MS (EI, *m/z*): calcd. for $C_{28}H_{20}N_2O_2$: 416.1, found 461.3. Elemental analysis, calcd (CHN): C, 80.75; H, 4.84; N, 6.73; found: C, 80.62.45; H, 4.92; N, 6.71.

2.6 Fabrication process of DSSCs using Doctor Blade's method.

The TiO_2 paste was prepared by adding 3.00 mL ethanol, 0.5 mL concentrated acetic acid to 1.00 g of TiO_2 nanoparticle (10-20 nm). The mixture was vigorously stirred and sonicated until a white pasty substance was obtained. A conductive glass (ITO) was washed two times by absolute ethanol then a clear tape is applied on a conductive face of ITO to draw a border of TiO_2 paste and fix the thickness of the paste between 50-60 nm. A few drops of TiO_2 paste were applied on the conductive surface of ITO and flattened by the doctor blade method. The homogenous layer of TiO_2 was annealed at 400℃ for 45 minutes by using a hot plate and then cooled at room temperature for 15 minutes.

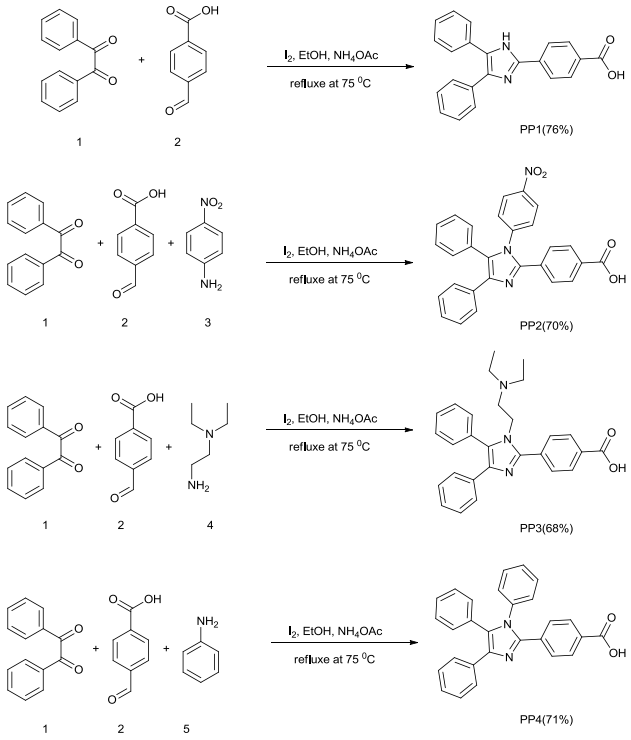

Scheme 1: Synthetic route for **PP1**, **PP2**, **PP3**, and **PP4** sensitizers.

The counter electrode (ITO with TiO_2) was immersed into a solution of synthesized dye (ethanol : THF, 5 :1) for 2 hours, figure 1, then rinsed with ethanol to remove the aggregate dye. The counter electrode was prepared by sketching the graphite by pencil on the conductive surface of another ITO glass.

The electrolyte solution was prepared by using 0.50 M KI, 0.05 M I_2 in ethylene glycol, and acetonitrile with a volume ratio of 4 : 1. A few drops of the electrolyte solution were added to the surface of TiO_2 and then the counter electrode was combined with the working electrode by using a binder clip and finally tested by photon incident beam to measure the efficiency of the prepared solar cell.[2]

3. Result and discussion

3.1 Syntheses

Four different substituted imidazole derivatives dyes were synthesized according to a previous literature method [30] and scheme 1 was shown the synthesis of these compounds. The electron-donating and electron-withdrawing groups were used as substituents on the imidazole by using cyclo condensation reaction between aldehyde and benzil in presence of ammonium acetate and iodine as a

catalyst. The mechanism of the reaction was carried out by using the iodine molecule to bond with the oxygen of aldehyde and that used to increase the reactivity of the carbonyl group by formation the diamine intermediate [30]. All the products were purified by recrystallization and characterized by 1H NMR and mass spectroscopy. The yields of all products are around 70%.

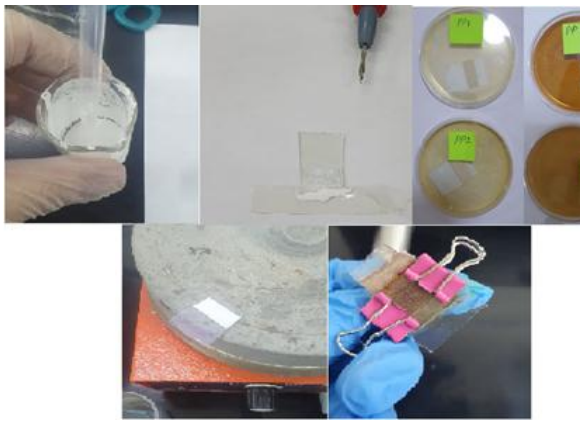

Figure 1: The fabrication process of DSSCs .

The UV-Vis spectra of all dyes were investigated in EtOH as a solvent and were shown in figure 2. All dyes exhibit a major absorption band between 329-335 nm. These absorption bands were ascribed of localization aromatic π-π* transition and table 1 was summarized the corresponding data. Noticeably, the dye **PP2** has a clearly high molar extinction coefficient (17200 M^{-1} cm^{-1}) and a stronger absorption band than other dyes which indicates that has a good ability for light harvesting. This result could be attributed to donating and accepting groups between imidazole and nitrobenzene respectively. The optical energy gap ($E_{g,opt}$) was essentially estimated by using the Einstein-Plank equation (equation 1) and **PP2** has the lowest optical energy gap (2.96 eV) if compared with other dyes which means that has a good electron transition from HOMO to LUMO than other dyes.

$$Eg, opt = 1240/\lambda onset \quad \ldots\ldots\ldots(1)$$

Where λ_{onset} is the onset of absorption spectra on the low energy side.

3.2 Optical properties:

Table 1: The optical properties and simulation energy for all synthesized dyes.

Dye	λ_{max}/nm	ε/M^{-1} cm^{-1}[a]	$E_{g,opt}$/eV	HOMO/eV[b]	LUMO/eV[b]	E_g/eV[b]
PP1	329	6000	3.35	-5.77	-2.53	3.24
PP2	333	17200	2.96	-6.05	-3.46	2.58
PP3	330	6400	3.18	-5.72	-2.43	3.29
PP4	329	7900	3.36	-5.74	-2.48	3.26

[a] Extinction coefficient (given from $A=\varepsilon cl$)

[b] Values obtained by computational study (DFT calculation)

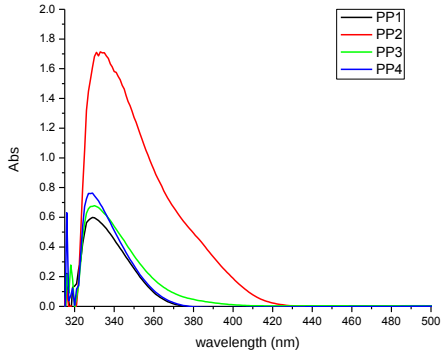

Figure 2: The absorption spectra of **PP1**, **PP2**, **PP3**, and **PP4** dyes (EtOH 1×10^{-4} M)

3.3 Computational studies

All dyes are calculated in vacuum at density functional theory (DFT) B3LYP by using the 6-311G* as a basis set for optimization geometry and frequency calculations [31]. There are no generated imaginary frequencies in all computational calculations which are indicated that the optimized structures are true energy minima. The electron distribution of the highest occupied molecular orbital (HOMO) and lowest unoccupied molecular orbital (LUMO) are shown the localization of electrons between donor and acceptor parts in the molecule. As shown in figure 3 , the HOMOs in all dyes are mainly distributed at the auxiliary donor area (phenyl-imidazole unit), while the LUMOs are localized on nitrobenzene for **PP2** dye and acceptor area (benzoic acid) for **PP1**, **PP3**, and PP4 which could lead to

giving best electron injection efficiency between the dye and TiO_2 surface. The dihedral angle between imidazole ring and benzoic acid in **PP1**, **PP2**, **PP3**, and **PP4** is 2.34°, 0.31°, 26.5°, and 1.20° respectively. So, **PP3** could be shows good solubility and better anti-aggregation on the surface of TiO_2 due to the steric effect between molecules and that leads to improving the efficiency of the DSSCs.

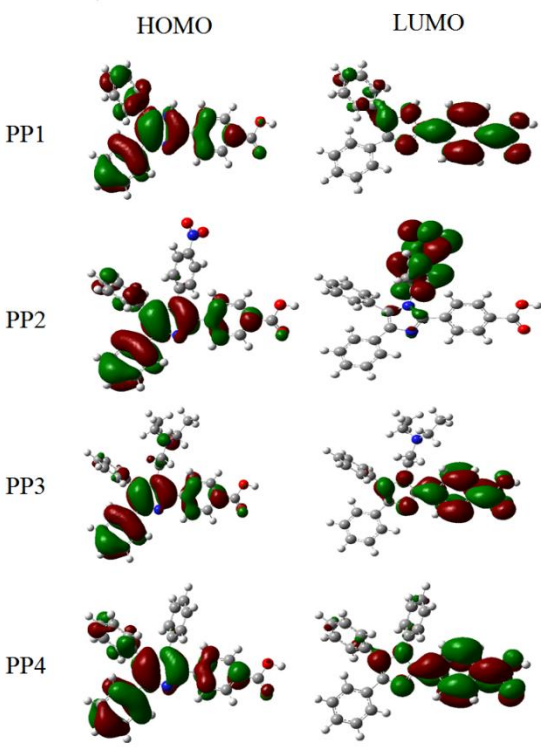

Figure 3: HOMOs and LUMOs for all dyes, predicted by DFT calculation.

3.4 DSSCs test

The performances of the solar cells are investigated by SMU unit, Ketly 2450 (simulator), and all dyes were measured under standard condition AM 1.5 at 100 mW cm^{-2}. The open-circuit voltage (V_{oc}) and short circuit current (J_{sc}) were calculated from the *J-V* curve. The fill factor (FF) and efficiency of the solar cells were determined using the following equations:

$$FF = (Imax\ Vmax)/(Jsc\ Voc) \quad \text{.....(2)}$$

$$\eta = (Jsc\ Voc\ FF)/Io \quad \text{.....(3)}$$

Where I_{max} is the maximum power point current, V_{max} is the maximum power point voltage of the solar cell, and I_0 is the total incident irradiance.

The *J-V* curve for all dyes is shown in figure 4 and the values of J_{sc}, V_{oc}, *FF*, and PCE are shown in table 2. In comparison between dyes, the highest PCE was represented with **PP3** dye and that could be attributed to the solubility of the dye due to their alkyl chain that bonded with N of imidazole ring which is prevent the aggregation of the dye on the surface of TiO_2. While, the lowest PCE was represented with **PP2** and this result could be due to the electron distribution of LUMO which is concentrated on nitrobenzene instead of benzoic acid and that could prevent the injection of an electron from dye to the TiO_2. The **PP2** dye has exhibited the lowest PCE and J_{sc} value when compared to that of **PP1**, **PP3**, and PP4 compounds, which could be attributed to the short electron lifetime and separation of LUMO from the acceptor group of the dye

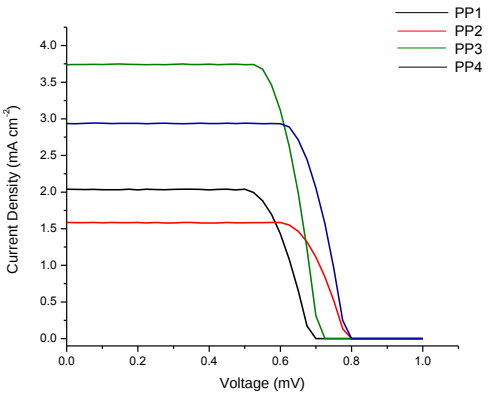

Figure 4: *J-V* curve of DSSCs sensitized by **PP1**, **PP2**, **PP3**, and **PP4**.

Table 2: photovoltaic parameters for all dyes under standard condition.

Dye	*Jsc* (mA cm^{-2})	*Voc* (mV)	*FF* (%)	PCE (%)
PP1	2.03	0.700	73.6	1.05
PP2	1.59	0.800	61.6	0.960
PP3	3.75	0.730	73.9	2.01
PP4	2.91	0.790	76.7	1.78

4. Conclusion

In this study, a series of four organic dyes based on an imidazole ring was designed and synthesized as a donor, π-bridge, and acceptor groups to apply in DSSCs. Furthermore, to investigate the efficiency of the solar cells by using different types of substitutions group on imidazole ring. These groups have enhanced the solubility by minimizing the aggregation of the dye. Interestingly, the PP2 dye has the lowest energy gap (2.55 eV) and lowest PCE value 0.96% (Jsc = 1.59 mA cm-2, Voc = 0.080 mV, FF = 61.6%), and that could be attributed to the electron distribution on LUMO which is delocalized on the nitrobenzene instead of benzoic acid part and that is effective to the efficient of the electron injection from the dye to the surface of TiO2. On the other hand, PP3 has the best efficiency of 2.01% (Jsc = 3.75 mA cm-2, Voc = 0.73 mV, FF = 73.9%) and that could be attributed to the excellent solubility of the dye and good electron distribution of HOMO and LUMO.

5. Acknowledgment

We thank the University of Karbala and the Al-Karkh University of science for funding and support.

6. References;

[1] B.C. Thompson, J.M.J. Fréchet, Polymer–Fullerene Composite Solar Cells, Angewandte Chemie International Edition, 47 (2008) 58-77.

[2] S.M. Abdalhadi, A.Y. Al-Baitai, H.A. Al-Zubaidi, Synthesis and Characterization of 2,3-Diaminomaleonitrile Derivatives by One-Pot Schiff Base Reaction and Their Application in Dye Synthesized Solar Cells, 2020, 21 (2020) 9.

[3] M. Cariello, S.M. Abdalhadi, P. Yadav, J.-D. Decoppet, S.M. Zakeeruddin, M. Grätzel, A. Hagfeldt, G. Cooke, An investigation of the roles furan versus thiophene π-bridges play in donor–π-acceptor porphyrin based DSSCs, Dalton Transactions, 47 (2018) 6549-6556.

[4] Z. Xu, C. Liu, S. Zhao, S. Chen, Y. Zhao, Molecular Sensors for NMR-Based Detection, Chem. Rev., 119 (2019) 195-230.

[5] H.-C. Gee, C.-H. Lee, Y.-H. Jeong, W.-D. Jang, Highly sensitive and selective cyanide detection viaCu2+ complex ligand exchange, Chemical Communications, 47 (2011) 11963-11965.

[6] X.-H. Zhu, J. Peng, Y. Cao, J. Roncali, Solution-processable single-material molecular emitters for organic light-emitting devices, Chemical Society Reviews, 40 (2011) 3509-3524.

[7] M.A. Baldo, M.E. Thompson, S.R. Forrest, High-efficiency fluorescent organic light-emitting devices using a phosphorescent sensitizer, Nature, 403 (2000) 750-753.

[8] H. Sirringhaus, 25th anniversary article: organic field-effect transistors: the path beyond amorphous silicon, Advanced materials, 26 (2014) 1319-1335.

[9] H. Chen, W. Zhang, M. Li, G. He, X. Guo, Interface engineering in organic field-effect transistors: Principles, applications, and perspectives, Chem. Rev., 120 (2020) 2879-2949.

[10] K.A. Mazzio, C.K. Luscombe, The future of organic photovoltaics, Chemical Society Reviews, 44 (2014) 78-90.

[11] G.P. Kini, S.J. Jeon, D.K. Moon, Design principles and synergistic effects of chlorination on a conjugated backbone for efficient organic photovoltaics: a critical review, Advanced Materials, 32 (2020) 1906175.

[12] M.K. Nazeeruddin, P. Péchy, T. Renouard, S.M. Zakeeruddin, R. Humphry-Baker, P. Comte, P. Liska, L. Cevey, E. Costa, V. Shklover, L. Spiccia, G.B. Deacon, C.A. Bignozzi, M. Grätzel, Engineering of Efficient Panchromatic Sensitizers for Nanocrystalline TiO2-Based Solar Cells, J. Am. Chem. Soc., 123 (2001) 1613-1624.

[13] L. Han, A. Islam, H. Chen, C. Malapaka, B. Chiranjeevi, S. Zhang, X. Yang, M. Yanagida, High-efficiency dye-sensitized solar cell with a novel co-adsorbent, Energy & Environmental Science, 5 (2012) 6057-6060.

[14] K. Kakiage, Y. Aoyama, T. Yano, K. Oya, J.-i. Fujisawa, M. Hanaya, Highly-efficient dye-sensitized solar cells with collaborative sensitization by silyl-anchor and carboxy-anchor dyes, Chemical Communications, 51 (2015) 15894-15897.

[15] H. Mohammadian-Sarcheshmeh, R. Arazi, M. Mazloum-Ardakani, Application of bifunctional photoanode materials in DSSCs: A review, Renewable and Sustainable Energy Reviews, 134 (2020) 110249.

[16] D.K. Kumar, J. Kříž, N. Bennett, B. Chen, H. Upadhayaya, K.R. Reddy, V. Sadhu, Functionalized metal oxide nanoparticles for efficient dye-sensitized solar cells (DSSCs): A review, Materials Science for Energy Technologies, 3 (2020) 472-481.

[17] P. Semalti, S.N. Sharma, Dye sensitized solar cells (DSSCs) electrolytes and natural photo-sensitizers: a review, Journal of nanoscience and nanotechnology, 20 (2020) 3647-3658.

[18] O. Adedokun, K. Titilope, A.O. Awodugba, Review on natural dye-sensitized solar cells (DSSCs), International Journal of Engineering Technologies IJET, 2 (2016) 34-41.

[19] Ö. Birel, S. Nadeem, H. Duman, Porphyrin-based dye-sensitized solar cells (DSSCs): a review, (2017).

[20] J. Gong, J. Liang, K. Sumathy, Review on dye-sensitized solar cells (DSSCs): Fundamental concepts and novel materials, Renewable and Sustainable Energy Reviews, 16 (2012) 5848-5860.

[21] M. Hosseinnezhad, R. Jafari, K. Gharanjig, Characterization of a green and environmentally friendly sensitizer for a low cost dye-sensitized solar cell, Opto-Electronics Review, 25 (2017) 93-98.

[22] S.M. Abdalhadi, Synthesis and study of new organic and organometallic compounds with photovoltaic applications, in, University of Glasgow, 2017.

[23] A. Mishra, M.K.R. Fischer, P. Bäuerle, Metal-Free Organic Dyes for Dye-Sensitized Solar Cells: From Structure: Property Relationships to Design Rules, Angewandte Chemie International Edition, 48 (2009) 2474-2499.

[24] G. Chidichimo, L. Filippelli, Organic solar cells: problems and perspectives, International Journal of Photoenergy, 2010 (2010).

[25] D. Kumar, K. Justin Thomas, C.-P. Lee, K.-C. Ho, Organic dyes containing fluorene decorated with imidazole units for dye-sensitized solar cells, The Journal of organic chemistry, 79 (2014) 3159-3172.

[26] S. Ashraf, J. Akhtar, H.M. Siddiqi, A. El-Shafei, Thiocyanate-free ruthenium (ii) sensitizers with a bi-imidazole ligand in dye-sensitized solar cells (DSSCs), New Journal of Chemistry, 41 (2017) 6272-6277.

[27] X. Chen, C. Jia, Z. Wan, X. Yao, Organic dyes with imidazole derivatives as auxiliary donors for dye-sensitized solar cells: Experimental and theoretical investigation, Dyes and Pigments, 104 (2014) 48-56.

[28] J. Sivanadanam, I.S. Aidhen, K. Ramanujam, New cyclic and acyclic imidazole-based sensitizers for achieving highly efficient photoanodes for dye-sensitized solar cells by a potential-assisted method, New Journal of Chemistry, 44 (2020) 10207-10219.

[29] Z. Wan, L. Zhou, C. Jia, X. Chen, Z. Li, X. Yao, Comparative study on photovoltaic properties of imidazole-based dyes containing varying electron acceptors in dye-sensitized solar cells, Synthetic metals, 196 (2014) 193-198.

[30] M. Kidwai, P. Mothsra, V. Bansal, R.K. Somvanshi, A.S. Ethayathulla, S. Dey, T.P. Singh, One-pot synthesis of highly substituted imidazoles using molecular iodine: A versatile catalyst, Journal of Molecular Catalysis A: Chemical, 265 (2007) 177-182.

[31] M.J. Frisch, G.W. Trucks, H.B. Schlegel, G.E. Scuseria, M.A. Robb, J.R. Cheeseman, G. Scalmani, V. Barone, G.A. Petersson, H. Nakatsuji, X. Li, M. Caricato, A.V. Marenich, J. Bloino, B.G. Janesko, R. Gomperts, B. Mennucci, H.P. Hratchian, J.V. Ortiz, A.F. Izmaylov, J.L. Sonnenberg, Williams, F. Ding, F. Lipparini, F. Egidi, J. Goings, B. Peng, A. Petrone, T. Henderson, D. Ranasinghe, V.G. Zakrzewski, J. Gao, N. Rega, G. Zheng, W. Liang, M. Hada, M. Ehara, K. Toyota, R. Fukuda, J. Hasegawa, M. Ishida, T. Nakajima, Y. Honda, O. Kitao, H. Nakai, T. Vreven, K. Throssell, J.A. Montgomery Jr., J.E. Peralta, F. Ogliaro, M.J. Bearpark, J.J. Heyd, E.N. Brothers, K.N. Kudin, V.N. Staroverov, T.A. Keith, R. Kobayashi, J. Normand, K. Raghavachari, A.P. Rendell, J.C. Burant, S.S. Iyengar, J. Tomasi, M. Cossi, J.M. Millam, M. Klene, C. Adamo, R. Cammi, J.W. Ochterski, R.L. Martin, K. Morokuma, O. Farkas, J.B. Foresman, D.J. Fox, Gaussian 16 Rev. C.01, in, Wallingford, CT, 2016.